

# Low temperature sintering and crystallisation behaviour of low loss anorthite-based glass-ceramics

CHUNG LUN LO, JENQ GONG DUH\*

*Department of Materials Science and Engineering, National Tsing Hua University, Hsinchu 300, Taiwan*  
*E-mail: jgd@mse.nthu.edu.tw*

BI SHIOU CHIOU

*Department of Electronics Engineering and Institute of Electronics, National Chiao Tung University, Hsinchu 300, Taiwan*

Anorthite-based glass-ceramics including  $\text{TiO}_2$  as nucleating agent were melted and quenched in this study. The effect of particle size on the sintering behaviour of glass powders was investigated in order to obtain low-temperature sintered glass-ceramics. Anorthite glass-ceramic starts to densify at the transition temperature of glass ( $T_g = 770^\circ\text{C}$ ) and is fully sintered before the crystallisation occurrence ( $880^\circ\text{C}$ ). Therefore, a dense and low-loss glass-ceramic with predominant crystal phase of anorthite is achieved by using fine glass powders ( $D_{50} = 0.45 \mu\text{m}$ ) fired at  $900^\circ\text{C}$ . The as-sintered density approaches 99% theoretical density and the apparent porosity is as low as 0.05 Vol%. The dense and crystallized anorthite-based glass-ceramic exhibits a fairly low dielectric loss of  $4 \times 10^{-4}$  at 1 MHz and a thermal expansion coefficient of  $4.5 \times 10^{-6}^\circ\text{C}^{-1}$ . Furthermore, the microwave characteristics were measured at 10 GHz with the results of  $K = 9.8$ ,  $Q_f = 2250$ , and temperature coefficient of resonant frequency  $\tau_f = -30 \text{ ppm}/^\circ\text{C}$ . © 2003 Kluwer Academic Publishers

## 1. Introduction

Due to the high frequency transmission of signals for wide applications in the wireless communications and computer fields, low dielectric constant, low temperature co-fired ceramics (LTCC) package have been developed to achieve the requirements of high signal propagation speed, good reliability and low cost [1–3]. “Low temperature” means that ceramic substrates should be sintered at less than  $1000^\circ\text{C}$  in order to be cofired with copper ( $1083^\circ\text{C}$ ), silver ( $961^\circ\text{C}$ ), or gold ( $1061^\circ\text{C}$ ). Several material systems such as glass plus ceramics [4, 5] and glass-ceramics have been developed to meet the requirements in applications for LTCC.

Glass-ceramics formed by controlled crystallisation of glass, are materials of high crystallinity grade. Properties such as lower dielectric constant, appropriate thermal expansion coefficient and cofirability with other materials, make glass-ceramic compatible with the high-performance multilayer ceramic substrates [6, 7]. Anorthite ( $\text{CaO} \cdot \text{Al}_2\text{O}_3 \cdot 2\text{SiO}_2$ ) based glass-ceramic system has been investigated and regarded as a potential material in LTCC substrates [8, 9]. In the fabrication of desirable glass-ceramic material used in LTCC substrates, the sintering or the com-

plete densification stage is proceeded by nucleation and binder burn-off, and followed by crystallisation [6]. If crystallisation occurs before sintering is nearly complete, the viscosity increases to near infinity and sintering then stops. When this occurs, products with good sinterability and high quality will be excluded. Hence, it is essential to understand the sintering and crystallisation behaviours of the glass-ceramics system in order to fabricate reliable LTCC devices and then to control their properties.

Several studies have been conducted on the nucleation and crystallization of anorthite glass-ceramic [10–12], and some are related to the low-temperature sintering behaviour of anorthite [13, 14]. The main purpose of the study is to gain a better understanding of the sintering and crystallisation behaviours in the anorthite-based glass-ceramic with various particle size distributions. The influence of particle size distribution on sintering to optimize the firing procedures for anorthite-based glass-ceramic powders was investigated. In addition, the dielectric properties at 1 MHz and at the microwave frequency (10 GHz) for anorthite glass-ceramics were also evaluated by using submicron-scale size glass powders sintered at temperatures below  $950^\circ\text{C}$ .

\* Author to whom all correspondence should be addressed.

## 2. Experimental procedures

The starting glass was of anorthite ( $\text{CaAl}_2\text{Si}_2\text{O}_8$ ) composition—18.16 CaO, 32.94  $\text{Al}_2\text{O}_3$ , 38.90  $\text{SiO}_2$  and 10.00  $\text{TiO}_2$  (wt%).  $\text{TiO}_2$  was added as nucleation agent. A glass batch of homogeneous mixture was prepared by ball milling and then melted in a Pt crucible at  $1650^\circ\text{C}$  for 10 hrs. To prevent the occurrence of any crystallisation, the melting substance was quenched into deionized water. The as-quenched glass was ground and screened through a 325-mesh stainless-steel wire screen to derive glass powders with particle size less than  $44\ \mu\text{m}$ . By controlling ball-milling time with zirconia media (2 mm in diameter) in deionized water, glass powders of different particle-size distribution were obtained. The particle-size distributions of powders were determined using laser light diffraction particle sizer (LS230, Coulter, U.S.A.). The median particle sizes of the ball-milled powders in this study were 1.5, 0.75, 0.6 and  $0.45\ \mu\text{m}$ . The evaluated particle-size distributions are shown in Fig. 1.

These powders were granulated by mixing in a 2.5 wt% poly vinyl alcohol (PVA) solution, and then pressed into pellets with 10 mm in diameter and 4 mm thick. The green density was  $65 \pm 2\ \text{Vol}\%$ . Pellets were sintered in air over a range of  $870\text{--}960^\circ\text{C}$  for 0.5 h at a heating rate of  $5^\circ\text{C}/\text{min}$ .

The fired bulk density and apparent porosity of the fired specimens were measured by Archimedeian immersion method using water as media with the accuracy of  $\pm 0.001\ \text{g}/\text{cm}^3$ . A differential thermal analyzer (DTA: DTA1600, Du Pont, U.S.A.) was used to study the crystallisation behaviour and to determine the glass transition temperature,  $T_g$ . The DTA instrument was previously calibrated by using Al, Ag and Zn, with well-determined melting temperatures. The DTA analysis was carried out under a flowing atmosphere of dry air ( $50\ \text{cm}^3/\text{min}$ ). Glass powders were then heated at a rate of  $5^\circ\text{C}/\text{min}$  up to  $1100^\circ\text{C}$  with a reference material of  $\alpha$ -alumina powders. The sintering behaviour was investigated using a dilatometer (DIL 402C, NETZSCH, Germany) at a heating rate of  $5^\circ\text{C}/\text{min}$  in air (flow rate of  $50\ \text{cm}^3/\text{min}$ ). The coefficient of thermal expansion was measured using a thermal analyzer (TMA

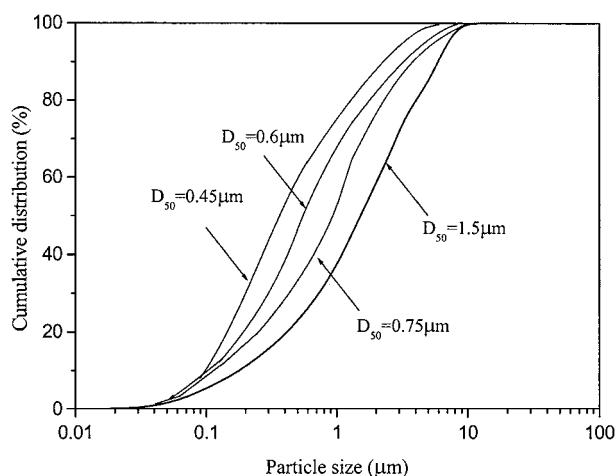


Figure 1 Particle-size distribution of ball-milled glass powders (where  $D_{50}$  is the median particle size).

SSC-5000, Seiko, Japan) in the temperature range of  $25\text{--}300^\circ\text{C}$ .

Phase identification of sintered specimens was performed by powder X-ray diffraction (XRD: D/MAX-B, Rigaku, Japan) with a wavelength of  $\text{Cu K}\alpha$  ( $\lambda = 1.5406\ \text{\AA}$ ). The scanning rate was 2 theta/min.

The dielectric characteristics were measured using Ag electrodes in a LCR meter (HP4284A, Hewlett-Packard, U.S.A.). In the microwave frequency range, the dielectric characteristics ( $K$  and  $Q_f$  value) were measured by Hakki-Coleman dielectric resonator method with a network analyzer (HP 8720C, Hewlett-Packard, U.S.A.) in  $S_{21}$  transmission mode. A cylindrically shaped specimen with an aspect ratio of 0.5 was positioned between two silver plates [15]. The dielectric properties including dielectric constant  $K$  and the loss  $\tan \delta$  were calculated from the frequency of the  $\text{TE}_{011}$  resonant mode [16].

## 3. Results and discussion

### 3.1. Crystallisation behaviour

The DTA traces recorded for anorthite-based glass powders of different median particle size are shown in Fig. 2. Since transition temperature of glass,  $T_g$ , is determined by a change in expansion behaviour, there will be an associated shift in heat capacity behaviour. The expansion of materials is a result of increase in the mean atomic vibration amplitude between atoms, and this vibration is the mechanism of thermal energy storage [17, 18]. For this reason,  $T_g$  can be measured using DTA and will appear as an endothermic trend with increasing temperature, as shown in Fig. 2. The convention

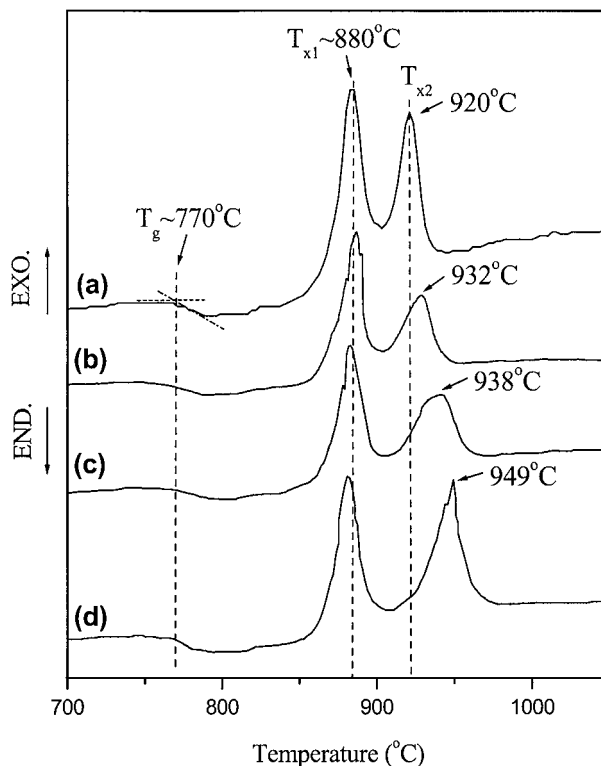


Figure 2 DTA records of anorthite-based glass powders with various median particle size (a)  $0.45\ \mu\text{m}$ , (b)  $0.6\ \mu\text{m}$ , (c)  $0.75\ \mu\text{m}$ , and (d)  $1.5\ \mu\text{m}$ .

for determining the glass transition temperature is to extend the straight-line portions of the baseline and the linear portion of the upward slope, marking their intersection. It is observed that initially all anorthite-based glass powders exhibit a transition of glass around 770°C ( $T_g$ ), followed by two exothermic transformations, corresponding to crystallisation from the glass.

DTA measurements were supplemented by XRD to identify crystal phases. Fig. 3 presents the corresponding XRD patterns for as-quenched glass and powders treated at various temperatures. As the firing temperature was raised up to 860°C, crystal phase of anorthite ( $\text{CaO} \cdot \text{Al}_2\text{O}_3 \cdot 2\text{SiO}_2$ ) was observed. However, the other crystal phase of perovskite ( $\text{CaTiO}_3$ ) was not shown up until the temperature increased above 910°C. As a result, the first exothermal peak,  $T_{x1}$ , in DTA curve (Fig. 2) was caused by the crystallisation of anorthite and the next smaller exothermal peak,  $T_{x2}$ , was related to perovskite crystallisation from the glass. Therefore, the non-isothermal heat-treatment is expected to produce a relative large amounts of anorthite and a small amounts of perovskite, as shown in Fig. 3. This observation is in agreement with Topping and Richard's study [19], in which the predominant and major crystal phase was anorthite in glass of  $\text{CaO} \cdot \text{Al}_2\text{O}_3 \cdot 2\text{SiO}_2$  nucleated with  $\text{TiO}_2$ .

It appears that peak temperatures of anorthite ( $T_{x1}$ ) in DTA for glass powders with various particle size distributions are almost identical and close to 880°C. This gives the evidence that the crystallisation mechanism for anorthite phase growth from the glass nucleated with  $\text{TiO}_2$  is bulk crystallisation dominated [20]. However, the other exothermal peak temperature for perovskite

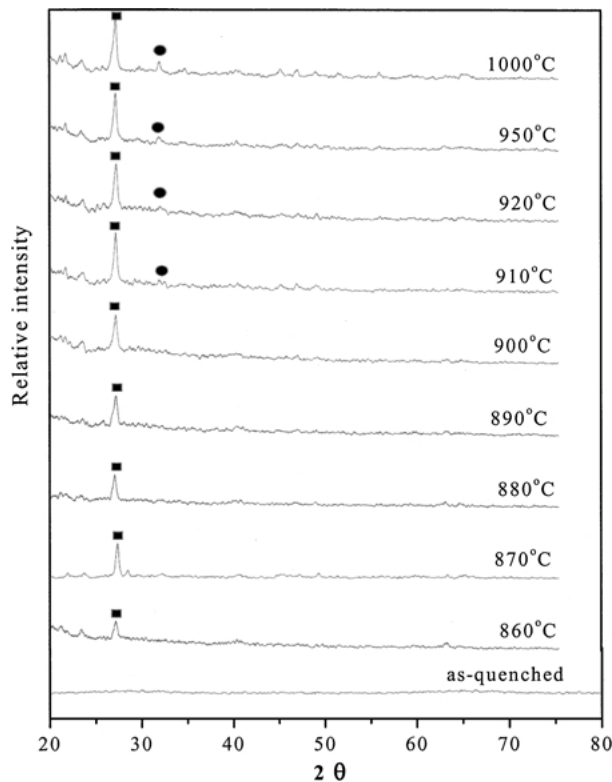


Figure 3 XRD patterns for as-quenched glass and powders treated at various temperatures (■: anorthite; ●: perovskite).

crystallisation,  $T_{x2}$ , is shifted to higher temperature as the median particle size increases. This implies that surface crystallization takes place. As a result, the addition of 10 wt%  $\text{TiO}_2$  as nucleating agent renders the glass powder to exhibit a sufficient efficiency of anorthite nucleation, and thus anorthite-based glass powders with bulk crystallisation at low temperature were achieved. This is, in fact, an important factor in controlling the reliability of LTCC products.

### 3.2. Sintering properties

For sintering at a constant heating rate of 5°C/min, the linear shrinkage of the specimens with different median particle size can be evaluated using dilatometric measurement. Fig. 4 shows the corresponding shrinkage curves with respect to (a)  $D_{50} = 1.5 \mu\text{m}$ , (b)  $D_{50} = 0.75 \mu\text{m}$ , (c)  $D_{50} = 0.6 \mu\text{m}$  and (d)  $D_{50} = 0.45 \mu\text{m}$ , where  $D_{50}$  is the median particle size of powders. It is evident that the specimen contraction is initially rapid at 770°C, which is congruent with the glass transition temperature  $T_g$  determined by DTA. It is believed that during the firing process for glass powders, sintering occurs by viscosity flow.

However, the shrinkage rate becomes sluggish as approaching near-full density. The densification rate ( $dL/dt$ ) reaches its maximum and starts to decrease at the saddle point (880°C) of curve (e) in Fig. 4, which is equal to the peak temperature of anorthite crystallisation ( $T_{x1}$ ) determined by DTA. This indicates that the

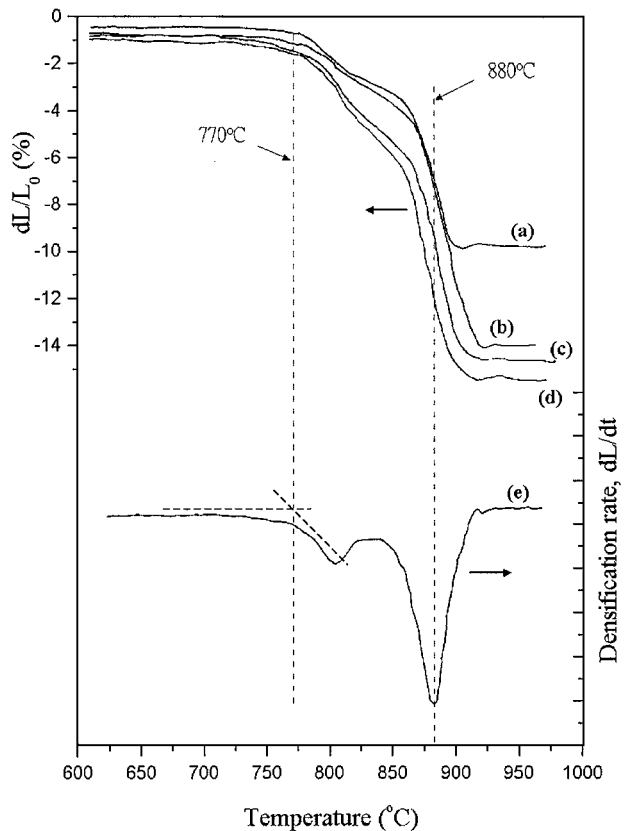


Figure 4 Dilatometric curves of anorthite based glass powders with the median particle size of (a) 1.5  $\mu\text{m}$ , (b) 0.75  $\mu\text{m}$ , (c) 0.6  $\mu\text{m}$ , and (d) 0.45  $\mu\text{m}$ , and (e) the derivative curve ( $dL/dt$ ) of powders with the median particle size of 0.45  $\mu\text{m}$ .

occurrence of crystallisation would degrade the densification rate. On the basis of the above results, it appears that the effective densification can be achieved from 770°C ( $T_g$ ) to 880°C ( $T_{x1}$ ) in this study.

For specimens undertaken the effective densification range from 770 to 880°C at a constant heating rate of 5°C/min (which means the duration time was identical for all specimens), the one with higher sintering rate would exhibit more feasibility to be fully densified than that with smaller sintering rate. If firing is carried out to complete densification, the fractional porosity originally present is equal to the volume shrinkage occurred during firing. For all unfired specimens, the green density was about 65 Vol%, and the probably maximum value of volume shrinkage was 35 Vol%, which is equivalent to 12% of linear shrinkage if isotropic shrinkage is assumed. In Fig. 4, the linear shrinkage in anorthite based glass with various particle size of (a) 1.5  $\mu\text{m}$ , (b) 0.75  $\mu\text{m}$ , (c) 0.6  $\mu\text{m}$  and (d) 0.45  $\mu\text{m}$  is evaluated to be 10, 13.8, 14.2 and 15%, respectively. The measured shrinkage in the range of 10–15% is quite closed to the estimated value of 12% as mentioned above. In fact, for powders with smaller median particle size, the less porosity and near-full dense glass-ceramic could be obtained.

The sintered densities of the specimens as a function of firing temperature are plotted in Fig. 5 with respect to various particle size. Examination of sintered specimens show that the sample with the larger size, such as 1.5 and 0.75  $\mu\text{m}$ , exhibits 3.4 and 6.8 Vol% porosity or 92.6 and 95.8% theoretical density, respectively. Only for glass powders with a median particle size of 0.45  $\mu\text{m}$ , a final state with a relative theoretical density of 99.0% and apparent porosity less than 0.05 Vol% can be achieved at temperature lower than 880°C. Theoretical

density (2.86 g/cm<sup>3</sup>) of the specimen was calculated from the ideal mineral composition [14].

The optimum heat-treatment procedures for a dense and crystallized glass-ceramic could be developed by considering the following factors. (i) Transition temperature of glass,  $T_g$ : It determines the starting sintering temperature. In forming useful LTCC substrates, it is important that no sintering occurs before the complete binder burnout [6]. The binder decomposition temperature are usually in the range of 400–700°C. (ii) Crystallisation temperature ( $T_{x1}$ ): It determines the temperature that the crystal phase starts to grow. When crystallisation occurs, it would decrease the densification. Usually the crystallisation temperature must be below 950°C for LTCC application. (iii) Sintering rate: Whether glass-ceramic powders can be fully sintered before densification stops depends on the sintering rate. It is revealed that both factors (i) and (ii) contribute the temperature region for efficient densification.

In present study, anorthite-based glass powders have been evaluated in an efficient densification range from 770–880°C ( $T_g \sim T_{x1}$ ). This meets the requirements of factors discussed above and is suitable for using in LTCC substrates fabrication. Depending on different mechanism, the sintering rate, i.e. factor (iii), usually exhibits the complex relationship with temperature, time, surface energy, viscosity, diffusivity . . . etc. [21]. Most of these parameters are interacted with each other and it is thus rather difficult to control without changing the original designed properties in glass-ceramic. In general, time is not a critical variable for process control, since it is impracticable in industry to improve the properties by merely prolonging the sintering time. Thus, more focuses are directed to decrease the particle size to improve the sintering rates [22], and to obtain reproducible processing and densification for the desired properties.

Full densification specimens can be achieved before the occurrence of anorthite crystallisation at 880°C in this work using submicron-scale glass powders. A completely sintered glass-ceramic with anorthite phase is obtained between 900–950°C. The crystallisation behaviour is illustrated with the aid of a DTA curve as shown in Fig. 6a, and the overall heat-treatment procedures are suggested in Fig. 6b. It should be noted that the heating rates would change the glass transformation temperature  $T_g$  and crystallisation temperature of glass powders. Thus, densification region may be different depending on heating rates of the heat-treatment. The corresponding particle size distribution for complete sintering would also be modified.

### 3.3. Dielectric properties of sintered samples

Fig. 7 presents the correlations between the dielectric property and sintered specimens with various particle distributions. The dependence of dissipation loss on the particle size is also indicated. It is revealed that only dense glass-ceramic shows a low loss and better dielectric property. The major contributor to dielectric loss is the porosity in specimen. In general, the dielectric constant would be underestimated for porous ones, since

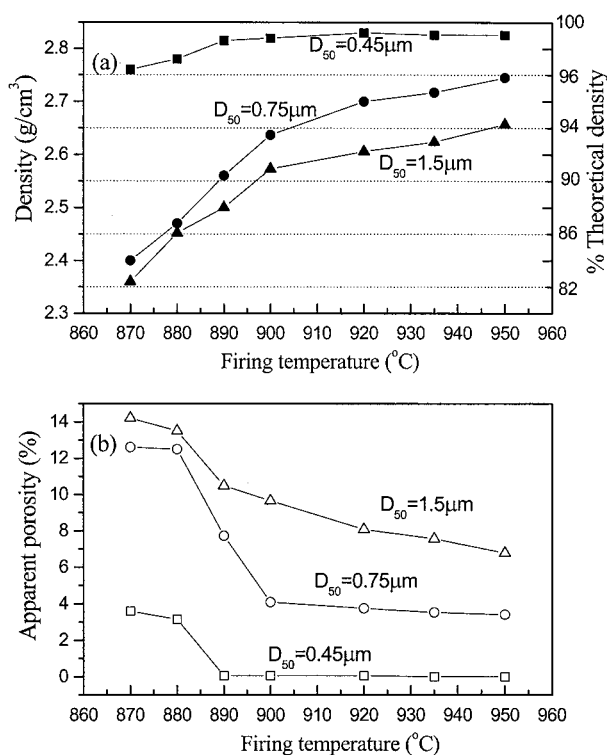


Figure 5 Bulk density and apparent porosity of fired specimens. ( $D_{50}$  indicates median particle size of glass powders.)

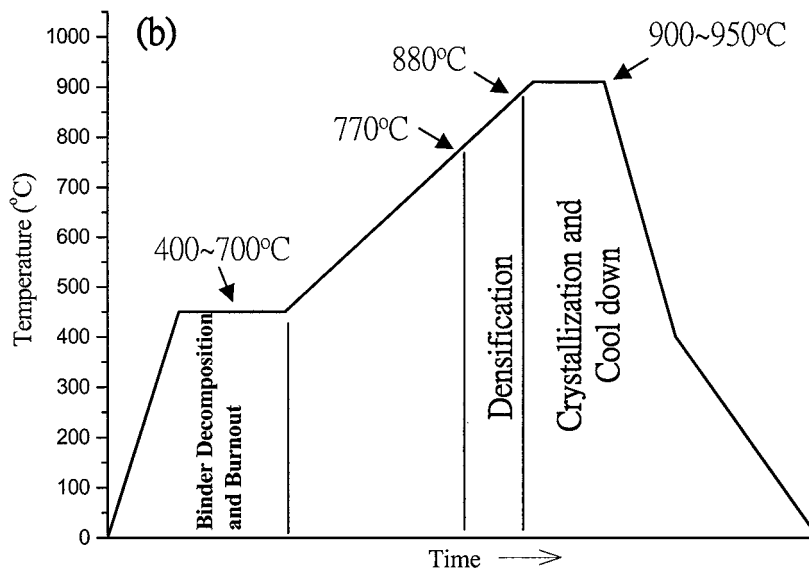
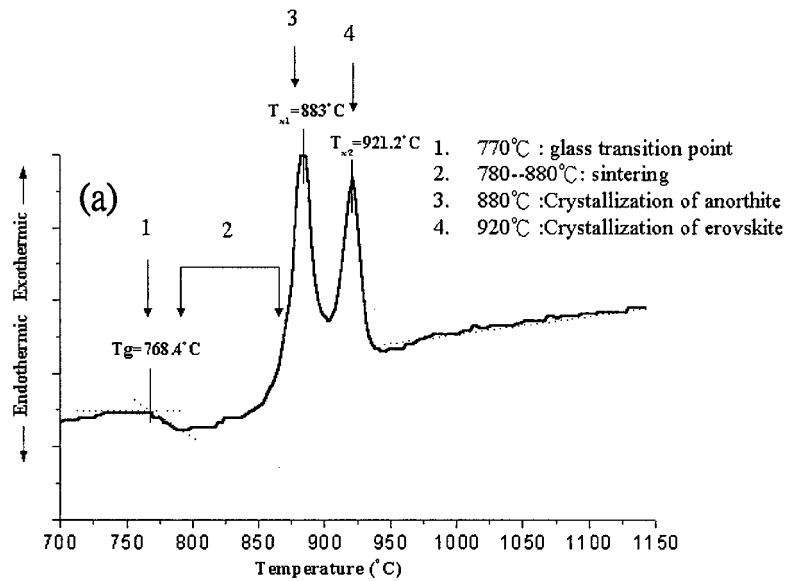


Figure 6 (a) A typical DTA curve for glass-ceramic powders; (b) the overall heat-treatment procedures.

the dielectric constant of the air in pores is assumed to be unity.

The well-sintered anorthite glass-ceramic exhibits the reliable dielectric properties. The dielectric loss of

0.0004 equals a high quality factor of 2500 at 1 MHz, which is very attractive in LTCC application. The thermal expansion coefficient is  $4.5 \times 10^{-6} \text{ } ^\circ\text{C}^{-1}$ , very close to that of Si ( $3.0 \times 10^{-6} \text{ } ^\circ\text{C}^{-1}$ ).

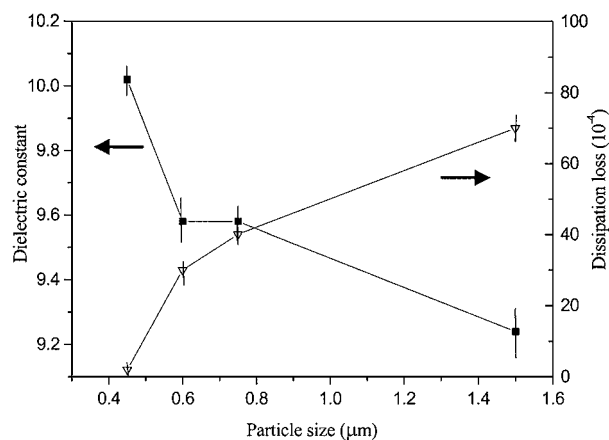


Figure 7 Dielectric properties of sintered anorthite-based glass-ceramic with various particle size.

TABLE I Properties of anorthite-based glass-ceramic

Composition (wt%)	
CaO	18.16
Al <sub>2</sub> O <sub>3</sub>	32.94
SiO <sub>2</sub>	38.90
TiO <sub>2</sub> (Nucleating agent)	10.00
Glass transformation temperature (°C)	770
Sintering temperature (°C)	900-950
Bulk density (g/cm <sup>3</sup> )	2.83
Relative theoretical density (%)	99%
Apparent porosity (Vol%)	0.05
Thermal expansion coefficient (°C <sup>-1</sup> )	$4.5 \times 10^{-6}$
Volum resistivity (Ω · cm)	$> 10^{13}$
Dielectric constant (at 1 MHz)	10.5
Dielectric loss (at 1 MHz)	0.0004
Dielectric constant (at 10 GHz)	9.8
Q <sub>f</sub> (at 10 GHz)	2250
τ <sub>f</sub> [-25°C-125°C] (ppm/°C)	-30

Microwave dielectric properties were measured at the resonant frequency of 10 GHz. The values of dielectric constant and  $\tan \delta$  are 9.8 and 0.00045 ( $Q_f = 2250$ ). The temperature coefficient of resonant frequency  $\tau_f$  are determined as  $-30$  ppm/ $^{\circ}\text{C}$  in the range from  $-55$  to  $125^{\circ}\text{C}$ . Table I lists the summarized characteristics of the anorthite-based ceramic. The overall dielectric and thermal expansion properties in addition to the process advantages are potentially attractive in LTCC application.

#### 4. Conclusions

The sintering and crystallisation behaviours for anorthite-based glass-ceramic were investigated with various particle size distributions. Complete sintering was achieved in the range from the glass transformation temperature ( $770^{\circ}\text{C}$ ) to crystallisation temperature ( $880^{\circ}\text{C}$ ) in glass-ceramic powders. The particle size plays an important role in the sintering rate, which is the crucial controlling parameter in achieving full densification. An optimized sintering profile for glass powders with anorthite composition containing 10 wt%  $\text{TiO}_2$  was established. In order to have full densification before crystallisation, it is necessary to decrease the particle size down to submicron scale to enhance the sintering. After complete sintering, the fully dense glass-ceramic with crystallised anorthite was successfully fabricated at relative low temperature. Superior and reliable properties such as low temperature sinterability, thermal expansion coefficient, and dielectric properties at 1 MHz and 10 GHz, were successfully derived in the dense specimen prepared from anorthite-based glass-ceramic powders.

#### Acknowledgments

This work is supported by the Philips Electronics Building Elements Industrial (Taiwan) Ltd. under contract No. C89054. Partial support from National Science Council under the contract No. NSC-89-2216-E009-038 is also appreciated.

#### References

1. R. R. TUMMALA, A. H. KUMAR and P. W. MCMILLAN, U.S. Patent no. 4301324, Nov. 17, 1981.
2. Y. SHIMADE, K. USTUMI, M. SUZUKI and H. TAKAMIZOWA, *IEEE Trans. Components, Hybrids Manuf. Technol.* **CHMT-6**(4) (1983) 382.
3. R. R. TUMMALA and E. J. RYMASZEWSKI, in "Microelectronic Packaging Handbook" (Van Nostrand-Reinhold, New York, 1989) p. 25.
4. K. NIWA, N. KAMEHARA, H. YOKOYAMA and KURIHARA, in "Multilayer Ceramic Circuit Board with Copper Conductor" (Westerville, OH, 1986) p. 41.
5. T. NORO and H. TOZAKI, Japanese Patent no. 6070799A (1986).
6. R. R. TUMMALA, J. U. KNICKERBOCKER, *et al.*, *IBM J. Res. Devel.* **36**(5) (1992) 889.
7. D. M. MATTOX, S. R. GURKOVICH, J. A. OLENICK and K. M. MASON, *Ceram. Eng. Sci. Proc.* **9**(11/12) (1988) 1567.
8. R. A. GUDLA, *Am. Ceram. Soc. Bull.* **50**(6) (1971) 555.
9. M. G. M. U. ISMAIL and H. ARAI, *J. Ceram. Soc. Jpn.* **100**(12) (1992) 1385.
10. N. P. PADTURE and H. M. CHAN, *J. Mater. Res.* **7**(1) (1992) 170.
11. H. C. PARK, S. H. LEE, M. M. SON, H. S. LEE and I. YASUI, *J. Mater. Sci.* **31** (1996) 4249.
12. C. LEONELLI, T. MANFREDINI, M. PAGANELLI, P. POZZI and G. C. PELLACANI, *ibid.* **26** (1991) 5041.
13. B. RYU and I. YASUI, *ibid.* **29** (1994) 3323.
14. Y. KOBAYASHI and E. KATO, *J. Amer. Ceram. Soc.* **77**(3) (1994) 833.
15. M. TAROU, *Electron. Ceram.* **21**(9) (1993) 38.
16. B. W. HAKKI and P. D. COLEMAN, *IRE Trans. Microwave Theory Tech.* **MTT-8** (1960) 4023.
17. W. D. KINGERY, H. K. BOWEN and D. R. UHLMANN, in "Introduction to Ceramics" (Wiley & Sons, New York, 1976) p. 93.
18. J. E. SHELBY, W. C. LACOURSE and A. G. CLAIRE, in "Engineering Properties of Oxide Glasses and Other Inorganic Glasses, Engineered Materials Handbook, Vol. 4: Ceramics and Glasses," S. J. Schneider, Technical Chairman (1991) p. 845.
19. J. A. TOPPING, *Ceram. Bull.* **56**(6) (1977) 574.
20. Z. STRAND, in "Glass-Ceramic Materials" (Elsevier, New York, 1995) p. 105.
21. M. N. RAHAMAN, in "Ceramic Processing and Sintering" (Marcel Dekker, New York, 1995) p. 392.
22. W. D. KINGERY, H. K. BOWEN and D. R. UHLMANN, in "Introduction to Ceramics" (John Wiley & Sons, New York, 1976) p. 476.

Received 29 May

and accepted 29 October 2002